Journal of Korean Powder Metallurgy Institute
Vol. 11, No. 2, 2004

Phase Transformation by the Oxidation of Air-passivated W and Mo Nanopowders Produced by an Electrical Explosion of Wires

Young Soon Kwon, Ji-Soon Kim, Alexander A. Gromov* and Moon-Hee Hong**

Research Centre for Machine Parts and Materials Processing, School of Materials and Metallurgical Engineering, University of Ulsan, San-29, Mugeo-2Dong, Nam-Ku, Ulsan 680-749, Korea,
Tel.82-52-259-2107, e-mail:yskwon@mail.ulsan.ac.kr
**Chemical Technology Department, Tomsk Polytechnic University, 30, Lenin Ave., Tomsk, 634050, Russia*
***Materials Science Division, Agency for Defence Development, P.O. Box 35-5, Yu-Sung, Daejeon, Korea*
(Received 15 March 2004 ; Accepted form 10 April 2004)

Abstract The passivation and oxidation process of tungsten and molybdenum nanopowders, produced by electrical explosion of wires was studied by means of FE-SEM, XPS, XRD, TEM, DTA-TGA and size distribution analysis. In addition, the phase transformation of W and Mo nanopowders under oxidation in air was investigated. A chemical process is suggested for the oxidation of W and Mo nano-particles after a comprehensive testing of passivated and oxidized powders.

Keywords : tungsten and molybdenum nanopowders, passivation, oxidation and coatings.

Nomenclature

EEW - electrical explosion of wires
DTA - differential-thermal analysis
TGA - thermogravimetric analysis
NP - nanopowders
UDP-4G - machine for obtaining NP by EEW
FESEM - field emission scanning electronic microscopy
BE - binding energy
XPS - X-ray photoelectron spectroscopy
a_s - average particle diameter, μm
S_{sp} - specific surface area, m^2/g
e/e_s - specific electrical energy liberated in the wire, a.u. (ratio of electrical energy liberated in the Mo(W) wire to the energy of sublimation of Mo(W))

[W], [O] ñ weight concentration of tungsten and oxygen, a.u.
ΔH_f^{298} (Me_xO_y) - enthalpy of oxides formation
SDA - size distribution analysis
BET - determination of S_{sp} by low temperature nitrogen adsorption (Brunauer- Emmet - Taylor method).

Introduction

Nanopowders (NP) of W and Mo synthesized by various methods such as evaporation-condensation, mechanochemical synthesis, sol-gel etc. are attractive for the synthesis of new composite materials for high-temperature applications[1]. One new promising method for the production of W and Mo nanopowders is the electrical explosion of wires (EEW)[2-3]. The metallic powders, produced by EEW, have a higher reactivity under sintering treatment than metallic NP synthesized under low-speed conditions[4]. The high reactivity of electroexplosive metallic NP can be correlated to their metastable state, since the formation of metastable W and Mo nanoparticles in the pulsed EEW process takes place under nonequilibrium conditions. The EEW method is characterized by a duration of 0.1 μs, a plasma temperature of about 10^4 K, a cooling rate of particles of up to 10^9 K/sec and a specific energy entering the wire of more than 1 MJ/kg[3].

It is the aim of this work to study origin of the EEW phenomenon and the mechanisms leading to the formation of superthin passivation layers on the metal-

lic particles produced by EEW. Data about passivation of W and Mo nano particles is poorly reviewed in literary sources. The majority of the papers regarding the passivation of particle surfaces provide information on reactive metals such as Al, Ti, Fe[5-8]. Oxidation of bulk W and Mo were studied in Ref.[9-11].

In this paper the results of DTA-TGA, XRD, SDA, TEM and FESEM-XPS studies on air-passivated electroexplosive W and Mo powders are presented, discussing the dynamics of oxidation. A chemical process being characteristic for the passivation of W and Mo NP and high-temperature oxidation in air is proposed.

Experimental Procedures

W and Mo NP were produced by EEW in Ar atmosphere and passivated in air. The physical properties and enthalpies of oxide formation for W and Mo are given in Table 1.

Powder production: The parameters of powder production are shown in Table 2. Production of W and Mo NP was carried out by using an EEW machine of the 5th generation UDP-4G, which was constructed for the mass production of metallic NP at University of Ulsan. The characteristics of the UDP-4G machine are comprehensively described elsewhere[12]. Among them, the high production speed of powders (~200 g/hour for W and Mo NP) should be particularly noted.

Powder passivation: The passivation operations for W and Mo powders were unified. Immediately after EEW nanopowders (m≈100 g after ~970 explosions) were collected in a steel container and placed into a hermetic box having room temperature and an argon gas pressure of 1.1 atm. Such conditions for air-passivation of metallic NP were discussed in a previous work[13]. Samples of preliminary mixed powders taken for the passivation of NP were analyzed by a number of methods (see below).

Powder analysis: DTA-TGA analysis of samples was carried out in a Paulik-Paulik-Erdey "Q-1500 D" derivatograph by heating up to 1300°C in air.

XRD analysis was performed using CuK_α radiation (Ni-monochromated) in a Rigaku "MAX-B" diffractometer. A 2θ-range of 30° to 120° was chosen.

The "Mastersizer 2000" by Malvern Instruments was used to obtain a size distribution curve. Prior to determining the size distribution, the powders were suspended in ethanol and ultrasonically treated for 15 minutes.

TEM studies on powders were carried-out using a "H-8100" (Hitachi, Japan). The powders were suspended in ethanol and air-dried before being investigated by TEM.

A "JSM-6500 F" (JEOL, Japan) FESEM-XPS apparatus was used for SEM studies. Powders were placed onto a glued foil and coated with a gold layer before being analyzed. C1s peaks at 284.5 eV caused by carbon contaminations of the samples were taken as a binding-energy reference. An estimated error of ±0.1 eV may be assumed for all measurements.

Results and Discussion

Table 1. Thermodynamic properties of W, Mo and their oxides.

Substance*	Density, m^2/g	Melting point, °C	Boiling point, °C	Enthalpy of formation, kJ/mole
W	19.3	3422	5555	0
WO_2	10.8	1500	1730	-585.3
WO_3	7.2	1473	1837	-836
Mo	10.3	2623	4639	0
MoO_3	4.7	795	1155	-744

*Web site: www.webelements.com

Table 2. Parameters of production for electroexplosive W and Mo.

NP	Voltage by EEW, kV	e/e_s, a.u.	Capacitance, μF	Inductivity, μH	Resistance, Ohm	Wire diameter, mm	Wire length, mm	Ar gas pressure, atm
W	22	1.1	2.17	0.35	0.07	0.2	37	1.5
Mo	24	1.4	2.17	0.35	0.06	0.3	57	1.5

Two samples of W and Mo NP (table 2) were produced by EEW under an Ar pressure of 1.5 atm. The Ar pressure, being higher than atmospheric, leads to the adsorption of Ar on the surface of particles. Adsorbed Ar prevents particle contact and sintering in the powder container. It also prevents an interaction between atmosphere gases and NP immediately after opening the machine to the atmosphere. Just after EEW the W and Mo NP contained about 4 % mass of adsorbed Ar. Although enthalpies of WO_3 and MoO_3 are relatively high (ΔH_f (WO_3) = -836 kJ/mole and $\Delta H_f(MoO_3)$ = -744 kJ/mole, table 1), there was no heat release during passivation of electroexplosive W and Mo NP as in Al NP having an enthaplphy of oxide formation of $\Delta H_f(Al_2O_3)$=-1675 kJ/mol[13]. The absence of heat liberation suggests that oxidation heat is dissipated inside the particles. Such a process is rather improbable since the values of thermal conductivity of W, Mo and Al do not significantly differ from each other. A more reasonable explanation may be the formation of oxides with lower oxygen content (such as W_3O and MoO) and post-oxidation to the highest degree of metal oxidation (WO_3 and MoO_3). The W and Mo NP were completely passivated in air within 25 hours, which is twice as fast as Al NP[14]. The passivation period was assumed to be finished when the powders stopped reacting with air, i. e. the gas mixture (Ar+0.1 vol. % air) pressure in the passivation chamber stopped decreasing.

Tungsten NP: According to the XRD data (Fig. 1), particles of passivated W NP contain three phases: α-W, β-W and W_3O. β-W formation is a characteristic feature for W NP, obtained by EEW. β-W has a lower density (19.1 g/cm^3) than α-W (19.3 g/cm^3, table 1). According to Tikhonov's XPS studies[14]* the finest W electroexplosive powder contains a higher concentration of β-W. In that work the W NP (sample produced under $e/e_s = 1.1$) was divided into 3 samples with S_{sp}=15.4 m^2/g, 2.8 m^2/g and 0.7 m^2/g. The quantity of β-W in the finest sample amounted to 43% mass. The sample with S_{sp} = 2.8 m^2/g contained traces of β-W. The sample with the lowest dispersity consisted completely of α-W. A possible reason for such a distribution of β-W in the samples with different S_{sp} is a higher cooling rate for the finest particles during EEW and a stabilization of crystal lattices of lower density.

W_3O peaks, registered by XRD (Fig.1) corresponded to the surface passivation layer. But according to XPS (Fig.2, viewed surface ~4000 μm^2), the oxygen content in the surface layers of particles was higher than for W_3O (ratio of weight concentrations [W]/[O]=34.5). It was calculated from the XPS data (Fig.2) that the composition of the surface layer is close to $WO_{1.6}$ (ratio of weight concentrations [W]/[O]=7.1), which is slightly higher than for WO_2 (ratio of weight concentrations [W]/[O]=5.8). A possible reason for such a difference between the XRD and XPS results is that well-crystallized W_3O covers the finest fraction of the powder, but the larger particles are covered by an amorphous oxide layer, which has a composition close to WO_2.

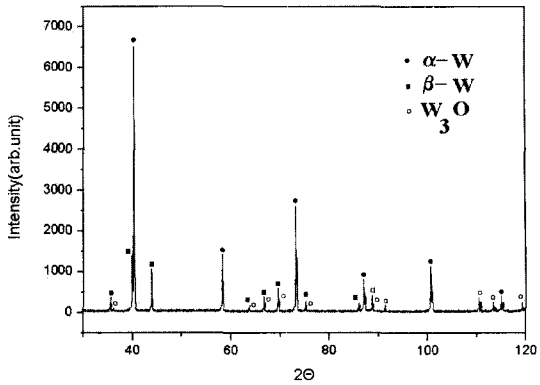

Fig 1. X-ray diffraction patterns of W nanopowder passivated by air (CuK_α radiation, λ=1.54056 nm).

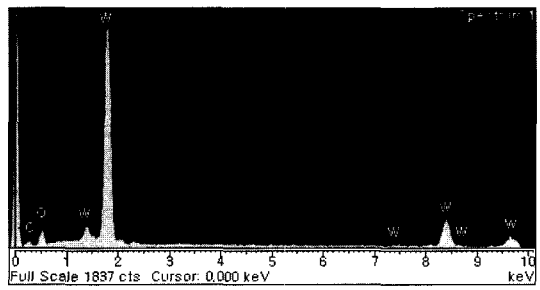

Fig. 2. FE-SEM/EDS pattern of W nanopowder passivated by air.

According to SDA, the W powder had a relatively narrow-size distribution in the range of 0.02 to 0.2 μm with a maximum at 0.06 μm (Fig. 3), which is in agreement with the SEM image in Fig. 2 and the TEM images in Fig. 4 a, b.

Passivated W nanoparticles produced in Ar-based gas media had nearly spherical shapes and smooth oxide layers (Fig. 2 and 4). The calculated thickness

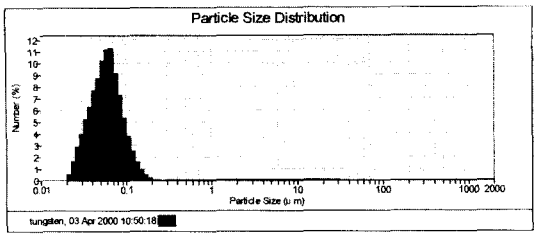

Fig. 3. Particle-size distribution of W nanopowder.

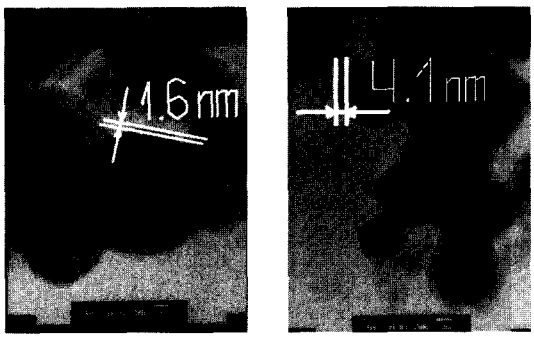

Fig. 4. TEM images of W nanopowder.

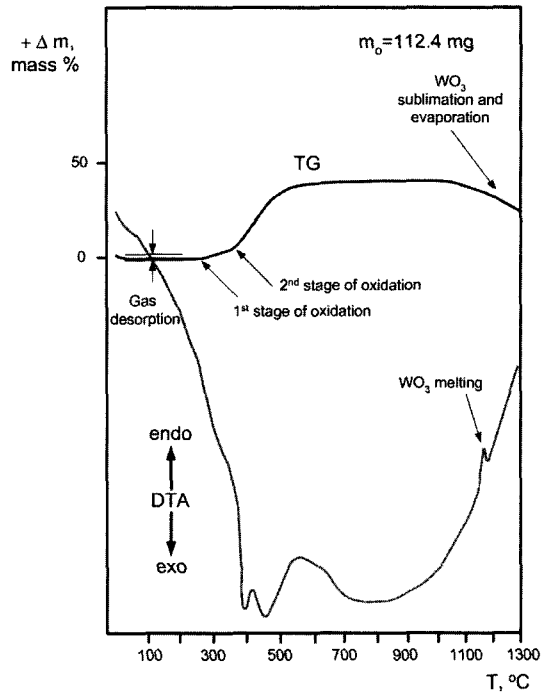

Fig 5. DTA-TGA curves of W nanopowder: m=112.4 mg, the heating rate in air is 15°C/min, and a-Al_2O_3 is the reference.

of the oxide layer (0.8 nm, Table 3) did not agree with the experimental value of 2.5 nm (see Fig. 4 b). Calculations of the thickness of the oxide layer on the particles (table 3) assumed a single particle diameter, but a powder having wide size distribution reveals stronger oxidization and a thicker passivation layer according to TEM micrographs in Fig. 4 b.

Fig. 5 represents the DTA-TGA curves of W NP under linear heating (15°C/min) up to 1300°C in air. Gas desorption occurred (2.2% mass decrease on a TG curve) during the heating of W NP from room temperature to 280°C. A DTA curve shows the exothermal peak from the very beginning of heating (Fig. 5). Possibly, gas desorption accompanied oxidation as in the case of Al NP[15]. The first stage of oxidation of W NP begins from 280°C up to 360°C (weight increase on a TG curve). The average mass rate of oxidation in the first stage was 0.6 mg O_2/min. Quantitative XRD analysis shows that the composition of the oxidized powder after the first stage was α-W (81% mass) and W_3O (19% mass). This stage of oxidation probably corresponds to an interaction of the finest W particles with oxygen, which is in agreement with the XRD data: β-W was completely oxidized (β-W peaks disappeared). The second stage of W oxidation continued up to 540°C (Fig. 5). The average mass rate of oxidation during the second stage was 1.1 mg O_2/min. After the second stage, oxidation of W NP led to complete W oxidation and WO_3 formation. There was no metallic W in the end products of oxidation up to 740°C. The content of metallic W in the initial NP calculated by a TG curve (Fig. 5) was 95.5 % mass.

Table 3. Characteristics for W NP produced by EEW and passivated by air.

NP	Temperature of the oxidation onset (TGA), °C	Temperature of the oxidation end (TGA), °C	*[W°]*, mass %	S_{sp} *(BET)*, m^2/g	Calculated a_s, nm	*[W_3O+$WO_{1.6}$]**, mass %	Calculated thickness of oxide layer, nm
W	280	740	95.5	3.9±0.3	79.1	2.2	0.8

**[W_3O+$WO_{1.6}$]=100 % − [W°] − [adsorbed gases].*

The products of complete oxidation consisted of lemon-yellow colored WO_3, of which the sublimation began at 990°C (weight decrease on a TG curve, fig.6). For the bulk WO_3 the sublimation temperature is a little lower (T_{subl}=900°C)[10]. Melting of WO_3 at a significantly lower temperature (1220°C, fig. 5) than for bulk WO_3 (1473°C, table 1) was also observed.

The possible chemical processes according to DTA/TGA/XRD data analyzing that took place during oxidation of W NP, produced by EEW, are shown in fig. 7.

To investigate the thermal stability of W NP to oxidation in humid air the powder was heated in 100% humid air up to 60°C and 120°C for 24 hours. Under these conditions the metal content decreased insignificantly (Table 4).

Molybdenum NP: As in the case of W NP, Mo powders had a narrow-size distribution with a maximum of 0.5 μm (Fig. 6). The SEM image of the Mo powders is presented in Fig. 8. Only the phase of metallic Mo is registered under XRD analysis of passivated Mo NP (Fig. 9). The content of metallic Mo in the passivated powder was 94.3% mass. But for the Mo powder the oxidation in air was more significant than for the W NP. Mo powder one month aged in air at room temperature already contained 87% mass of metallic Mo. The DTA-TGA curves of such powders are represented in Fig. 10. The content of adsorbed gases was 1.6% mass. Gas desorption occurred from the beginning of heating up to ~300°C. The simultaneous exotherm on a DTA curve assumes an oxidation process. A mass increase began at 310°C. Mo NP oxidizes in two macro-stages (first – 310-440°C, second – 440-640°C) (Table 5, Fig. 10, DTA curve).

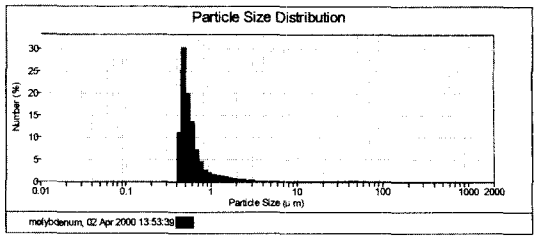

Fig 6. Particle-size distribution of Mo nanopowder.

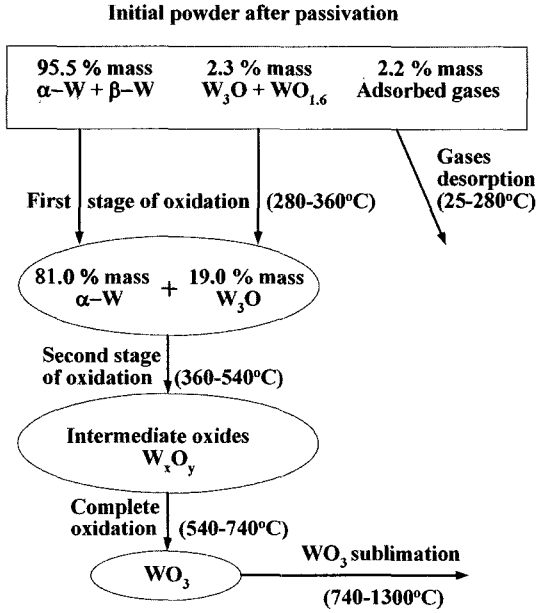

Fig 7. Chemical processes during oxidation of W nanopowder.

Melting of MoO_3 starts at 780°C (endo-peak on DTA

Table 4. W nanopowder thermal stability in air by passivation and ageing.

Powder state	[W°]
Fresh powder (0 hours)	96.0 % mass
Passivated powder (24 hours)	95.5 % mass
Aged powder (770 hours, 100 % humidity, 60°C)	95.3 % mass
Aged powder (770 hours, 100 % humidity, 120°C)	92.5 % mass

Table 5. Characteristics for Mo NP produced by EEW and passivated by air.

NP	Temperature of the oxidation onset (TGA), °C	Temperature of the oxidation end (TGA), °C	*[Mo°]*, % mass	S_{sp} *(BET)*, m^2/g	Calculated a_s, nm	*[Molybdenum oxides]**, mass %	Calculated thickness of oxide layer, nm
Mo	310	640	94.3	5.2±0.3	120.2	4.1	2.4

**[Molybdenum oxides]=100 % - [Mo°] ñ [adsorbed gases].*

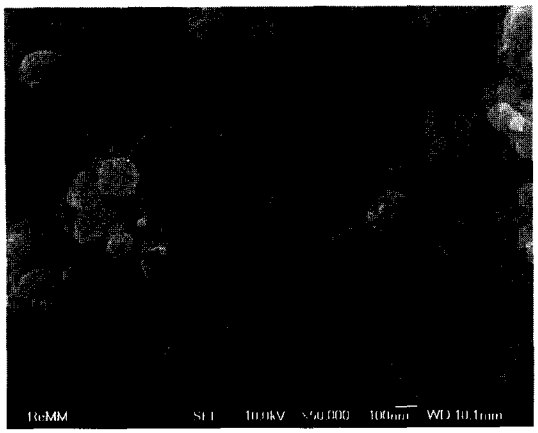

Fig 8. SEM image of Mo nanopowder passivated by air.

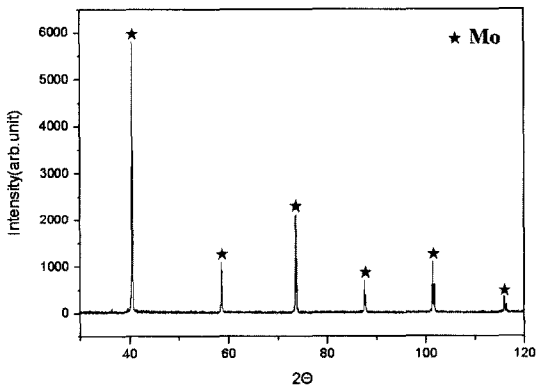

Fig 9. X-ray diffraction patterns of Mo nanopowder passivated by air (CuK_α radiation, λ=1.54056 nm).

curve). After MoO_3 melting two parallel processes were observed: MoO_3 evaporation (mass decrease on a TG curve) and rest Mo oxidation (exo-peak on a DTA curve).

Experiments on the thermal stability of Mo NP under oxidation in 100% humid air showed a decrease of metal content in Mo NP as shown in Table 6.

Conclusion

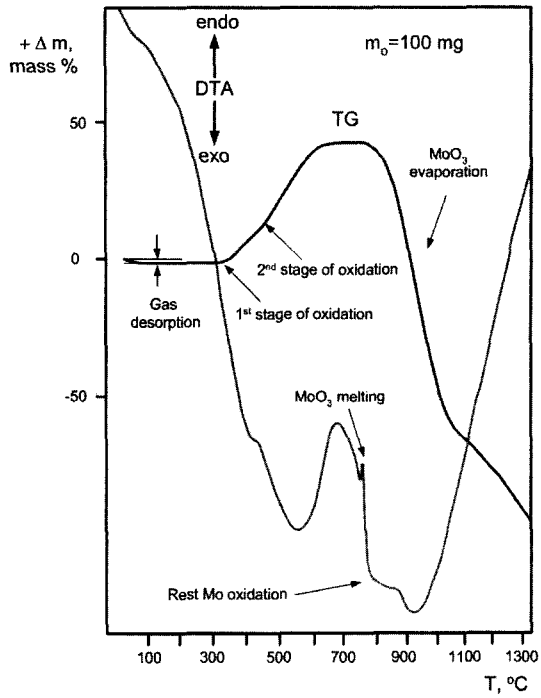

Fig 10. DTA-TGA curves of aged Mo nanopowder: m = 100 mg, the heating rate in air is 15°C/min, and α-Al_2O_3 is the reference.

Following results were obtained in the framework of these studies:

1. Mass production (~200 g/hour) of W and Mo nanopowders is possible with the EEW method. Metallic particles are spherical with a smooth surface and a diameter of less than 2 μm. An explosion of a W wire results in β-W phase formation. The content of β-W is higher in the finest fraction of nanopowder.

2. The passivation period of W and Mo nanopowders is ~25 hours. During this time an oxide coating of less than 2 nm thickness forms on metallic particles.

3. The composition of an oxide layer for W NP was W_3O for the finest fraction of the powder and close to WO_2 for the largest particles.

Table 6. Mo nanopowder thermal stability in air by passivation and ageing.

Powder state	[Mo°]
Fresh powder (0 hours)	95.3 % mass
Passivated powder (24 hours)	94.3 % mass
Aged powder (720 hours, 50 % humidity, room temperature)	87.0 % mass
Aged powder (770 hours, 100 % humidity, 60°C)	79.3 % mass
Aged powder (770 hours, 100 % humidity, 120°C)	76.8 % mass

4. W and Mo NP hold on their surface up to 3% mass of adsorbed gases. The temperature for intensive oxidation onset in air is 280°C for W NP and 310°C for Mo NP.

5. The possible chemical processes offered for W NP oxidation in air up to 740°C. Results show that the thermal stability of W NP in 100% humid atmosphere is higher than for Mo NP.

6. For Mo NP storage in air results in a sufficient decrease in metal content (from 94.3% mass for passivated powder to 87.8 % mass for 1-month aged powder).

Acknowledgements

This work has been supported by a cooperative research program of the Agency for Defence Development and the Korea Science and Engineering Foundation (KOSEF) through the Research Center for Machine Parts and Materials Processing (ReMM) at the University of Ulsan.

This paper is dedicated to Professor In-Hyung Moon in deep respect on the occasion of his retirement.

References

1. E. Ozawa, Y. Kawakami and T. Seto: Scripta mater. **44** (2001) 2279.
2. Weihua Jiang and Kiyoshi Yatsui: IEEE Transactions on Plasma Science **26** (1998) 1498.
3. Y. S. Kwon, A. P. Ilyin, D. V. Tikhonov, O. B. Nazarenko, and G. V. Yablunovskii: Current Status and Future Development of the Electroexplosive Technology / Proceedings. The 7th Korea-Russia Int. Symp. On Science and Technology (KORUSí2003). **1** (2003) 175-178.
4. T. A. Khabas: Glass and Ceramics **59** (2002) 404.
5. David E. G. Jones, Richard Turcotte, Robert C. Fouchard, Queenie S. M. Kwok, Anne-Marie Turcotte, and Zainab Abdel-Qader: Propellants, Explosives, Pyrotechnics **28** (2003) 120.
6. J. C. Sanchez-Lopez, A. Caballero and A. Fernandez: J. Eur. Ceram. Soc. **18** (1998) 1195.
7. L. I. Vergara, M. C. G. Passeggi, Jr. J. Ferron: Appl. Surf. Sci. **187** (2002) 199.
8. S. J Roosendaal, J. P. R Bakker, A. M. Vredenberg, F. H. P. M. Habraken,:Surf. Sci. **494** (2001) 197.
9. C. Agte and I. Vacek: Wolfram a Molybden, SNTL, Praha, (1954).
10. O. Kubaschewski and B. E. Hopkins: Oxidation of Metals, Butter Worths, London, (1962).
11. J. Benard: Oxidation des Metaux, Gauthier Villars Editeur, Paris, (1964).
12. V. Ya. Ushakov, A. P. Ilyin, O. B. Nazarenko, D. V. Tichonov and G. V. Yablunowskii: Ultrafine Powders Produced With Wire Electrical Explosion (Production and Properties), The First Korea-Russian Intern. Symp. on Sci. and Tech. Proc., University of Ulsan, Ulsan, (1997) 167.
13. Y. S. Kwon, Alexander A. Gromov, Alexander P. Ilyin, Geun-Hie Rim: Appl. Surf. Sci. **211** (2003) 57.
14. D. V. Tikhonov: Technical Science candidate thesis, Tomsk Polytechnic University, Tomsk, (2000).
15. A. P. Ilíin, A. A. Gromov and G. V. Yablunovskii: Comb. Expl. Shock Waves, **37** (2001) 418.